Flexural capacity model for RC beams strengthened with bolted side-plates incorporating both partial longitudinal and transverse interactions

Z.W. Shan and R.K.L. Su*

Department of Civil Engineering, The University of Hong Kong, Hong Kong, China

Abstract

Existing reinforced concrete (RC) beams with inadequate flexural capacity can be strengthened by bolting steel plates onto both sides of the face of beam. However, the effectiveness of these bolted side-plated (BSP) beams is affected by the mechanical slipping of bolts which is known as the partial interaction of the steel plates and the RC beam. To avoid overestimating the flexural capacity of the strengthened beam, the effects of partial interaction should be properly quantified in the structural design. Therefore, a new design model to determine the flexural capacity of BSP beams that takes into consideration both partial longitudinal and transverse interactions has been developed in this study. Strain and curvature factors are introduced to quantify the partial interaction. Based on these two factors, modified moment capacity equations are presented. The proposed model is then validated by comparing the analytical results with the test results from another study. Finally, a simplified design method is

* corresponding author, email: klsu@hku.hk

proposed based on the results of a parametric study.

Keywords: Reinforced concrete beams; Bolted side-plate; Partial transverse interaction; Longitudinal interaction; Strain factor; Curvature factor; Design method.

1. Introduction

Structural deterioration, usage changes or amended design specifications and safety requirements may require the enhancement of the load-carrying capacity of structural elements. It is well recognized that lightly reinforced concrete (RC) beams can be effectively strengthened by bolting bottom plate. However, for moderately reinforced beams, this method can lead to over-reinforcement problem and significant reduction in ductility capacity. On the other hand, using bolted side plate method to strengthen RC beams, the side plate can be extended from tensile to compression zone and can act as both tension and compression reinforcement. Thus the over-reinforcement problem can be avoided and the flexural capacity of beam can be greatly enhanced without losing ductility capacity [1-2]. During the past few years, many researchers have conducted comprehensive studies of this strengthening method due to its convenience in construction and cost effectiveness [3-15].

However, partial interaction caused by bolt slipping remains a key issue that needs to be resolved when designing bolted side-plated (BSP) beams. The strain profile of a BSP beam with full interaction (or in other words, without any bolt slipping) is shown in Fig. 1(b). The strain profiles of the longitudinal and partial transverse interactions are presented in Figs. 1(c) and 1(d). It can be seen that the longitudinal and transverse slips lead to the reduction of longitudinal deformation and curvature of the steel plate

compared to those of full interaction.

Oehlers et al. [8] developed fundamental mathematical models for partial transverse interaction and further determined the number of connectors required to resist transverse forces and limit the amount of partial transverse interaction in BSP RC beams. Nguyen et al. [7] obtained the longitudinal slip strain induced by both longitudinal and partial transverse interactions and examined the neutral axis separation between the steel plate and RC beams. A realistic model was developed to describe the longitudinal slip and neutral axis separation by Nguyen et al. [16]. Zhu and Su [14] evaluated the strength of BSP coupling beams with a mixed analysis method and rigid plastic analysis (RPA). Their results showed that partial interaction has considerable effects on the flexural capacity of the strengthened coupling beams. Although the aforementioned studies have provided the basis for further investigation of partial interaction, they have not quantified the effects of partial interaction on the flexural capacity of strengthened BSP beams.

Su et al. [17] investigated the longitudinal interaction in BSP RC beams under different load conditions. Li et al. [18] and Su et al. [19] studied the transverse interaction in BSP RC beams by using a piecewise linear transverse shear transfer model. Siu and Su [10] introduced strain and curvature factors to represent longitudinal and partial transverse interactions. Based on these two factors, Lo et al.

[20] assumed that longitudinal and partial transverse interactions are independent and proposed optimum strain and curvature factors for calculating the flexural capacity of BSP beams. However, the longitudinal and partial transverse interactions are not independent because the latter can cause more longitudinal slippage between the steel plates and RC beams. Hence, the effects of partial transverse interaction on partial longitudinal interaction should not be ignored.

In this study, a theoretical study is conducted which takes into account the effects of partial transverse interaction on partial longitudinal interaction. Strain and curvature factors are derived to quantify the effects of partial interaction. Furthermore, moment capacity equations (MCEs) are modified to incorporate these two factors. To validate their effectiveness, the flexural capacities obtained from various strain factors and those from the RPA are compared with test results from a previous study. A parametric study is conducted based on the proposed theoretical model, and a simplified design method for BSP beams is proposed.

2. Theoretical model

The theoretical model for quantifying the effects of the partial interaction of simply supported BSP beams under four-point, three-point and uniformly distributed loading as illustrated in Fig. 2 is derived in this section. As the formulations of the

theoretical model for these three loading cases are quite similar, only the formulation of a BSP beam under four-point loading will be provided in detail here. Only the key results of the other two loading cases will be discussed.

2.1. Assumptions

The assumptions are summarized below.

(1) The behavior of the concrete component in BSP beams is linear elastic, which is used to deduce the strain and curvature factors;

(2) The distribution of the shear connector along the length of the beam is uniform, which means that the shear force and stiffness of the bolts are uniformly distributed along the longitudinal direction;

(3) The difference in the curvature between the steel plate and the concrete component varies linearly along the shear span and is kept constant in the pure bending zone. As the moments in the steel plate and the RC beam at the support are both equal to zero, the difference in curvatures of these two components is zero. The difference in the curvatures increases from the support to the loading point. The actual nonlinear profile of the curvature difference in a shear span is illustrated as a black solid curve in Fig. 3 which holds true even in the ultimate load condition [13]. The assumed linear profile allows a conservative estimation of the flexural load capacity as the curvature difference and hence the transverse

partial interaction effects are overestimated. This assumption was also adopted by Yuan [13] for analyzing the strengthened beams under three-point bending.

(4) The plane sections remain plane after loading;

(5) The ultimate strain is 0.003 [21];

(6) The equivalent rectangular stress block is applied, and the two coefficients in the equivalent rectangular stress block are both 0.85 [21]; and

(7) The centroid of the steel plate is lower than that of the RC beams.

2.2. Force in the bolts and slips

The internal forces of the BSP beams, steel plate and concrete component are illustrated in Fig. 4. The distributed shear force in the longitudinal (t_m) and transverse (v_m) directions can be derived based on the assumptions and equilibrium conditions:

$$t_m = \frac{dT_m}{dx} = \frac{K_b S_l}{S_b} = k_m S_l \tag{1}$$

$$v_m = \frac{dV_m}{dx} = \frac{K_b S_t}{S_b} = k_m S_t \tag{2}$$

where $K_b = \frac{R_{by}}{S_{by}}$ is the bolt stiffness which can be obtained from bolt shear tests, R_{by} is the yield shear strength of the bolt, S_{by} is the yield displacement of the bolt, S_l is the longitudinal slip between the steel plate and RC beam, $k_m = \frac{K_b}{S_b}$ is the bolt stiffness per unit length, S_b is the bolt spacing, T_m is the shear force in the bolts in the longitudinal direction, V_m is the shear force in the bolts in the transverse direction and S_t is transverse slipping between the steel plate and RC beam.

When the axial forces of the concrete and the steel plates are equated and the shear force of the bolt is in the longitudinal direction:

$$T_m = E_c A_c \varepsilon_{cc.c} = E_p A_p \varepsilon_{pc.p} \tag{3}$$

where E_c is the elastic modulus of the RC beam, E_p is the elastic modulus of the steel plate, A_c is the cross-sectional area of the RC beam, A_p is the cross-sectional area of the steel plate, $\varepsilon_{cc,c}$ is the strain at the centroid of the RC beam and $\varepsilon_{pc,p}$ is the strain at the centroid of the steel plate. Furthermore, the shear force in the bolts T_m in the longitudinal direction and the gradient of the slip $dS_l(x)/dx$ can be derived from Eq. (1) as:

$$T_m = k_m \int S_l dx \tag{4}$$

$$\frac{dS_l(x)}{dx} = \frac{1}{k_m} \cdot \frac{d^2 T_m}{dx^2} \tag{5}$$

2.3. Partial interaction under four-point bending

A simply supported BSP beam with a length L subjected to two equal and symmetrically arranged point loads with a distance of ξL from the supports (where $0 < \xi < 0.5$) is shown in Fig. 2(a). Due to symmetry, only the left half of the beam is considered in the partial interaction analysis.

2.3.1. Partial longitudinal interaction with full transverse interaction

Full transverse interaction means that the RC beam and steel plates have the same curvature. In this section, BSP beams with partial interaction in the longitudinal direction and full transverse interaction is considered. The effect of full transverse

interaction on longitudinal slip strain is shown in Fig. 5(b).

If a section with a distance of x from the left support as shown in Fig. 2(a) is considered, the equilibrium of the external and internal moments is expressed as:

$$M(x) = M_c(x) + M_p(x) + T_{m,tfi}(x) i_{cp} \tag{6}$$

where M_c is the moment resisted by the RC beam, M_p is the moment taken by the steel plate, M is the total external moment, $T_{m,tfi}$ is the axial tensile force in the steel plate and RC beam through partial longitudinal interaction, and i_{cp} is the separation of the neutral axial of the RC beam and centroid axis of the steel plate. The subscript *tfi* denotes full transverse interaction. The last term in the equation represents the additional coupling induced by the partial longitudinal interaction which causes axial tension $T_{m,tfi}$ in the steel plate and axial compression in the RC beams, both acting at their respective centroid.

Assuming that there is full transverse interaction, the curvature of the steel plate and RC beam is the same and can be expressed as follows:

$$\phi(x) = \frac{M_c(x)}{E_c I_c} = \frac{M_p(x)}{E_p I_p} \tag{7}$$

where $E_c I_c$ and $E_p I_p$ are the flexural stiffness of the RC beam and steel plates respectively, and ϕ is the curvature of the BSP beam. Substituting Eq. (7) into Eq. (6) provides:

$$\frac{M_c(x)}{E_c I_c} = \frac{M_p(x)}{E_p I_p} = \frac{M(x) - T_{m,tfi}(x) i_{cp}}{E_c I_c + E_p I_p} = \frac{M(x) - T_{m,tfi}(x) i_{cp}}{\sum EI} \tag{8}$$

where $\sum EI = E_c I_c + E_p I_p$ is the total flexural stiffness of the BSP beams. The longitudinal slipping at the centroid of the steel plate is given as:

$$S_l(x) = \delta_{pc,p}(x) - \delta_{pc,c}(x) \tag{9}$$

where $\delta_{pc,p}$ and $\delta_{pc,c}$ are the longitudinal displacement of the steel plate and RC beam at the centroid of the steel plate. By differentiating Eq. (9) with respect to x, the strain difference in the BSP beams is derived, as shown in Fig. 5(b).

$$\left(\frac{dS_l(x)}{dx}\right)_{tfi} = \varepsilon_{pc,p}(x) - \varepsilon_{pc,c}(x) \tag{10}$$

where $\varepsilon_{pc,p}$ and $\varepsilon_{pc,c}$ are, respectively, the strain of the steel plate and RC beam at the centroid of the steel plate, and $\varepsilon_{pc,c}$ can be obtained from Eq. (11).

$$\varepsilon_{pc,c}(x) = -\frac{T_{m,tfi}(x)}{E_c A_c} + i_{cp}\phi(x) \tag{11}$$

Using Eqs. (3), (7), (8) and (11), Eq. (10) becomes

$$\left(\frac{dS_l(x)}{dx}\right)_{tfi} = \left(\sum \overline{EA} + \frac{i_{cp}^{\ 2}}{\sum EI}\right) T_{m,tfi}(x) - \frac{i_{cp}}{\sum EI} \cdot M(x) \tag{12}$$

where $\sum \overline{EA} = \frac{1}{E_p A_p} + \frac{1}{E_c A_c}$. Substituting $\left(\frac{dS_l(x)}{dx}\right)_{tfi} = \frac{1}{k_m} \cdot \frac{d^2 T_{m,tfi}(x)}{dx^2}$ into Eq. (11) and letting $p^2 = k_m\left(\sum \overline{EA} + \frac{i_{cp}^{\ 2}}{\sum EI}\right)$ and $q = \frac{k_m i_{cp}}{\sum EI}$, the governing equation of the partial longitudinal interaction can be derived as:

$$\frac{d^2 T_{m,tfi}(x)}{dx^2} - p^2 \cdot T_{m,tfi}(x) + q \cdot M(x) = 0 \tag{13}$$

By applying the loading condition as shown in Fig. 2(a), the shear force *V* and moment *M* along the BSP beam can be expressed as:

$$V(x)=\begin{cases}F & 0\le x\le \xi L\\ 0 & \xi L\le x\le L/2\end{cases} \tag{14}$$

$$M(x)=\begin{cases}Fx & 0\le x\le \xi L\\ F\cdot \xi L & \xi L\le x\le L/2\end{cases} \tag{15}$$

where F is the external load. The piecewise functions that govern partial longitudinal interaction are derived by substituting Eq. (15) into Eq. (13):

$$\begin{cases}\dfrac{d^2T_{m,tfi}(x)}{dx^2}-p^2\cdot T_{m,tfi}(x)+q\cdot Fx=0 & 0\le x\le \xi L\\ \dfrac{d^2T_{m,tfi}(x)}{dx^2}-p^2\cdot T_{m,tfi}(x)+q\cdot F\cdot \xi L=0 & \xi L\le x\le L/2\end{cases} \tag{16}$$

The general solution of the above governing equation can be written as:

$$\begin{cases}T_{m1,tfi}(x)=A_1e^{px}+B_1e^{-px}+q\cdot\dfrac{Fx}{p^2} & 0\le x\le \xi L\\ T_{m2,tfi}(x)=A_2e^{px}+B_2e^{-px}+q\cdot\dfrac{F\cdot\xi L}{p^2} & \xi L\le x\le L/2\end{cases} \tag{17}$$

As it is assumed that there is uniform distribution of the shear connector along the length of the beam, the force in the bolt in the longitudinal direction should approach zero at the support. Due to symmetry, the longitudinal slip (S_l) at the mid-span should also be zero. Furthermore, the longitudinal slip and its gradient should satisfy the continuity conditions at the loading point. As $t_m=\dfrac{dT_{m,tfi}(x)}{dx}=k_mS_l(x)$ and $\dfrac{1}{k_m}\dfrac{d^2T_{m,tfi}(x)}{dx^2}=\dfrac{dS_l(x)}{dx}$, the boundary conditions of the axial tensile force can be written as:

$$\begin{cases} T_{m1,tfi}(0)=0 \\ T_{m2,tfi}{}'(\frac{L}{2})=0 \\ T_{m1,tfi}{}'(\xi L)=T_{m2,tfi}{}'(\xi L) \\ T_{m1,tfi}(\xi L)=T_{m2,tfi}(\xi L) \end{cases} \tag{18}$$

Substituting Eq. (17) into Eq. (18), the longitudinal force in the bolts become:

$$\begin{cases} T_{m1,tfi}(x)=\dfrac{Fq}{2p^3}\dfrac{(e^{p\xi L}+e^{2p\xi L})(e^{px}-e^{-px})}{e^{p\xi L}-e^{pL}}+\dfrac{Fqx}{p^2} & 0\le x\le \xi L \\ T_{m2,tfi}(x)=\dfrac{Fq}{2p^3}\dfrac{(e^{p\xi L}-e^{-p\xi L})(e^{px}+e^{pL-px})}{(e^{p\xi L}-e^{pL})}+\dfrac{Fq\cdot\xi L}{p^2} & \xi L\le x\le L/2 \end{cases} \tag{19}$$

2.3.2. Partial longitudinal interaction with partial transverse interaction

The above equations are derived based on the assumption that there is no partial transverse interaction between the RC concrete beam and steel plates. However, partial transverse interaction does in fact exist, and can cause a difference in the longitudinal slip strain between the two components as illustrated in Fig. 5(c). Assuming that the difference of the curvature between the beam and plate components is $\Delta\phi$, the curvature relation between the two components can be written as:

$$\Delta\phi(x)=\phi_c(x)-\phi_p(x) \tag{20}$$

where ϕ_c and ϕ_p are the curvature of the RC beam and steel plate respectively. As the flexural stiffness of the RC beam is much greater than that of the steel plate, when partial transverse interaction occurs, the curvature of the RC beams can be assumed to be the same as that of full transverse interaction (by neglecting the small increases in

the curvature of the RC beam). Hence Eq. (20) can be rewritten as:

$$\Delta\phi(x) = \phi(x) - \phi_p(x) \tag{21}$$

The change in the force in the bolt in the longitudinal direction from full to partial transverse interaction can be expressed as:

$$\Delta T_m(x) = T_{m,tfi}(x) - T_{m,tpi}(x) \tag{22}$$

where subscript *tpi* denotes the partial transverse interaction.

Consider a section with a distance of x from the left support with longitudinal and partial transverse interactions. Then, the cross-sectional moment $M(x)$ of the BSP beam can be expressed as:

$$M(x) = E_c I_c \phi(x) + E_p I_p \phi_p(x) + T_{m,tpi}(x) i_{cp} . \tag{23}$$

When there is partial longitudinal and full transverse interactions, from Eqs. (6) and (7), the moment $M(x)$ becomes:

$$M(x) = \phi(x) \sum EI + T_{m,tfi}(x) i_{cp} . \tag{24}$$

From Eqs. (21)-(24), the force in the bolts in the longitudinal direction under partial transverse interaction can be related to that under full transverse interaction by using the following equation:

$$T_{m,tpi}(x) = T_{m,tfi}(x) + \Delta\phi(x) \frac{E_p I_p}{i_{cp}} \tag{25}$$

In Eq. (25), the term $\Delta\phi(x) E_p I_p / i_{cp}$ represents the difference in the axial tensile

force due to the difference in the curvature $\Delta\phi(x)$ which will be solved in the next section. After taking into account the effect of partial transverse interaction on longitudinal slip strain, the longitudinal slip strain can be expressed as Eq. (26) (refer to Eq. (12) for a similar formulation).

$$\left(\frac{dS_l(x)}{dx}\right)_{tpi} = \left(\sum \overline{EA} + \frac{i_{cp}^{\ 2}}{\sum EI}\right) T_{m,tpi}(x) - \frac{i_{cp}}{\sum EI} \cdot M(x) \tag{26}$$

Replacing the term $T_{m,tpi}$ in Eq. (26) with Eq. (25), Eq. (26) becomes:

$$\left(\frac{dS_l(x)}{dx}\right)_{tpi} = \left(\sum \overline{EA} + \frac{i_{cp}^{\ 2}}{\sum EI}\right) T_{m,tfi}(x) - \frac{i_{cp}}{\sum EI} \cdot M(x) + \Delta\phi(x) \frac{E_p I_p}{i_{cp}} \left(\sum \overline{EA} + \frac{i_{cp}^{\ 2}}{\sum EI}\right) \tag{27}$$

The first two terms on the right hand side of Eq. (27) can be replaced with $\left(\frac{dS_l(x)}{dx}\right)_{tfi}$ in accordance with Eq. (12). Hence, Eq. (27) becomes

$$\left(\frac{dS_l(x)}{dx}\right)_{tpi} = \left(\frac{dS_l(x)}{dx}\right)_{tfi} + \Delta\left(\frac{dS_l(x)}{dx}\right) \tag{28}$$

where $\Delta\left(\frac{dS_l(x)}{dx}\right) = \Delta\phi(x) \frac{E_p I_p}{i_{cp}} \left(\sum \overline{EA} + \frac{i_{cp}^{\ 2}}{\sum EI}\right)$, and from the above analysis, it can be concluded that partial transverse interaction can cause an increase in the longitudinal slip strain between the RC beam and steel plate.

2.3.3. Partial transverse interaction

As the moments in the steel plate and the RC beam at the support are equal to zero, hence, the difference in the curvature of these two components is zero. The difference in the curvature increases from the support to the loading point. For simplicity, the difference in the curvature is assumed to increase linearly from the support to the

loading point and then kept constant to the mid-span, as shown in Eq. (28).

$$\begin{cases} \Delta\phi(x) = \dfrac{\Delta\phi_{\max} x}{\xi L} & 0 \le x \le \xi L \\ \Delta\phi(x) = \Delta\phi_{\max} & \xi L \le x \le L/2 \end{cases} \tag{28}$$

where $\Delta\phi_{\max}$ is the maximum curvature difference. Equation (28) is integrated twice, and the transverse slip between the two components is given by:

$$\begin{cases} S_{t1}(x) = \dfrac{\Delta\phi_{\max} x^3}{6\xi L} + C_1 x + C_2 & 0 \le x \le \xi L \\ S_{t2}(x) = \dfrac{x^2}{2}\Delta\phi_{\max} + C_3 x + C_4 & \xi L \le x \le L/2 \end{cases} \tag{29}$$

where C_{i} are the unknown coefficients to be determined. Due to the symmetry, the first derivation of the transverse slip is equal to zero at the mid-span. Moreover, the deformation compatibility (i.e. the transverse slip and its first derivation) should be satisfied at the loading point. Furthermore, the vertical force equilibrium of the steel plate provides another loading condition as shown below:

$$\int_0^L v_m(x)dx = 0 \tag{30}$$

The unknown coefficients can be determined by satisfying the aforementioned compatibility and loading conditions. Then, the transverse slip function can be expressed as:

$$\begin{cases} S_{t1}(x) = (\dfrac{x^3}{6\xi L} + (\dfrac{\xi L}{2} - \dfrac{L}{2})x + (\dfrac{\xi^3 L^2}{12} + \dfrac{L^2}{12} - \dfrac{\xi^2 L^2}{6}))\Delta\phi_{\max} & 0 \le x \le \xi L \\ S_{t2}(x) = (\dfrac{x^2}{2} - \dfrac{L}{2}x + (\dfrac{\xi^3 L^2}{12} + \dfrac{L^2}{12}))\Delta\phi_{\max} & \xi L \le x \le L/2 \end{cases} \tag{31}$$

Substituting Eq. (31) into $v_m(x) = k_m S_t(x)$, the transverse shear flow can be

derived as follows:

$$\begin{cases} v_{m1}(x) = k_m(\frac{x^3}{6\xi L} + (\frac{\xi L}{2} - \frac{L}{2})x + (\frac{\xi^3 L^2}{12} + \frac{L^2}{12} - \frac{\xi^2 L^2}{6}))\Delta\phi_{\max} & 0 \le x \le \xi L \\ v_{m2}(x) = k_m(\frac{x^2}{2} - \frac{L}{2}x + (\frac{\xi^3 L^2}{12} + \frac{L^2}{12}))\Delta\phi_{\max} & \xi L \le x \le L/2 \end{cases} \quad (32)$$

Eq. (32) is integrated and from the equilibrium conditions ($V(0) = 0$ and $V(\frac{L}{2}) = 0$) in the steel plate component, the transverse shear along the beam is obtained,

$$\begin{cases} V_{p1}(x) = k_m(\frac{x^4}{24\xi L} + (\frac{\xi L}{4} - \frac{L}{4})x^2 + (\frac{\xi^3 L^2}{12} + \frac{L^2}{12} - \frac{\xi^2 L^2}{6})x)\Delta\phi_{\max} & 0 \le x \le \xi L \\ V_{p2}(x) = k_m(\frac{x^3}{6} - \frac{L}{4}x^2 + (\frac{\xi^3 L^2}{12} + \frac{L^2}{12})x - \frac{\xi^3 L^3}{24})\Delta\phi_{\max} & \xi L \le x \le L/2 \end{cases} \quad (33)$$

Eq. (33) is integrated and from the boundary condition at the support when the moment is zero and satisfies the continuity at the loading point, the moment in the steel plate along the beam is derived as follows:

$$\begin{cases} M_{p1}(x) = M_{p1}'(x)\Delta\phi_{\max} & 0 \le x \le \xi L \\ M_{p2}(x) = M_{p2}'(x)\Delta\phi_{\max} & \xi L \le x \le L/2 \end{cases} \quad (34)$$

where $M_{p1}'(x) = k_m(\frac{x^5}{120\xi L} + (\frac{\xi L}{12} - \frac{L}{12})x^3 + (\frac{\xi^3 L^2}{24} + \frac{L^2}{24} - \frac{\xi^2 L^2}{12})x^2)$ and $M_{p2}'(x) = k_m(\frac{x^4}{24} - \frac{L}{12}x^3 + (\frac{\xi^3 L^2}{24} + \frac{L^2}{24})x^2 - \frac{\xi^3 L^3}{24}x + \frac{\xi^4 L^4}{120})$.

At the loading point, the equilibrium of the internal and external moments are considered:

$$F \cdot \xi L = M_{p1}(\xi L) + (\frac{M_{p1}(\xi L)}{E_p I_p} + \Delta\phi_{\max})E_c I_c + (T_{m,tfi}(\xi L) + \Delta\phi_{\max}\frac{E_p I_p}{i_{cp}})i_{cp} \quad (35)$$

From Eq. (35), $\Delta\phi_{\max}$ can be determined as:

$$\Delta\phi_{\max} = \frac{F \cdot \xi L - T_{m,tfi}(\xi L) \cdot i_{cp}}{E_c I_c} \frac{1}{\frac{1+\eta}{\eta} \cdot \frac{M_{p1}'(\xi L)}{E_c I_c} + (1-\eta)} \tag{36}$$

where $\eta = \frac{E_p I_p}{E_c I_c}$ denotes the ratio of the flexural stiffness of the steel plate to that of the RC beam.

2.3.4. Strain and curvature factors

To quantify the effects of partial interaction, the strain factor (α_ε) and curvature factor (α_ϕ) defined from Eqs. (37) and (38) are introduced [10].

$$\alpha_\varepsilon(x) = \frac{\varepsilon_{pc,p}(x)}{\varepsilon_{pc,c}(x)} \tag{37}$$

$$\alpha_\phi(x) = \frac{\phi_p(x)}{\phi_c(x)} \tag{38}$$

Substituting Eq. (10) into Eq. (37), the strain factor becomes:

$$\alpha_\varepsilon(x) = \frac{1}{1 - (\frac{dS_l(x)}{dx})_{tpi} \frac{1}{\varepsilon_{pc,p}(x)}} \tag{39}$$

where $(\frac{dS_l}{dx})_{tpi}$ can be determined from Eq. (27). The longitudinal strain in the steel plate at the centroid of the steel plate $\varepsilon_{pc,p}$ is determined from Eqs. (5) and (25), as given in Eq. (40).

$$\varepsilon_{pc,p}(x) = \frac{T_{m,tfi}(x) + \Delta\phi(x) \frac{E_p I_p}{i_{cp}}}{E_p A_p} \tag{40}$$

According to the relation between the moment and curvature together with Eq.

(20), the curvature factor can be rewritten as:

$$\alpha_{\phi}(x)=\frac{1}{1+\Delta\phi(x)\dfrac{E_pI_p}{M_p(x)}} \tag{41}$$

2.4. Partial interaction under three-point bending

A simply supported BSP beam subjected to a single point load with a distance ξL from the left support is shown in Fig. 2(b). The strain and curvature factors are determined by following the formulation for loading under four-point bending. Due to space restrictions, only the key results are presented here.

The moment distribution along the BSP beam under a single point load is:

$$M(x)=\begin{cases}(1-\xi)Fx & 0\le x\le \xi L\\ F(\xi L-\xi x) & \xi L\le x\le L\end{cases} \tag{42}$$

The boundary and continuity conditions are:

$$\begin{cases} T_{m1,tfi}(0)=0\\ T_{m2,tfi}(L)=0\\ T_{m1,tfi}{}'(\xi L)=T_{m2,tfi}{}'(\xi L)\\ T_{m1,tfi}(\xi L)=T_{m2,tfi}(\xi L)\end{cases} \tag{43}$$

The profile of the force in the bolt in the longitudinal direction is given as:

$$\begin{cases} T_{m1,tfi}(x)=A_1e^{px}+B_1e^{-px}+q\cdot\dfrac{(1-\xi)Fx}{p^2} & 0\le x\le \xi L\\ T_{m2,tfi}(x)=A_2e^{px}+B_2e^{-px}+q\cdot\dfrac{F\xi(L-x)}{p^2} & \xi L\le x\le L\end{cases} \tag{44}$$

where

$$A_1=\frac{Fq(e^{p\xi L}-e^{2pL-p\xi L})}{2p^3(e^{2pL}-1)}$$

$$A_2 = \frac{Fq(e^{p\xi L} - e^{-p\xi L})}{2p^3(e^{2pL} - 1)}$$

$$B_1 = \frac{Fq(e^{2pL - p\xi L} - e^{p\xi L})}{2p^3(e^{2pL} - 1)}$$

$$B_2 = \frac{Fq(e^{2pL - p\xi L} - e^{2pL + p\xi L})}{2p^3(e^{2pL} - 1)}$$

The difference in the curvature when linear variation is assumed is expressed as:

$$\begin{cases} \Delta\phi(x) = \dfrac{\Delta\phi_{\max} x}{\xi L} & 0 \le x \le \xi L \\ \Delta\phi(x) = \dfrac{\Delta\phi_{\max}(L - x)}{(1-\xi)L} & \xi L \le x \le L \end{cases} \tag{45}$$

Similar to loading under four-point bending, the continuity and loading conditions need to be considered. Hence, the transverse slip can be determined as:

$$\begin{cases} S_{t1}(x) = \dfrac{\Delta\phi_{\max} x^3}{6\xi L} + C_1 x + C_2 & 0 \le x \le \xi L \\ S_{t2}(x) = \dfrac{\Delta\phi_{\max}}{(1-\xi)L}\left(\dfrac{Lx^2}{2} - \dfrac{x^3}{6}\right) + C_3 x + C_4 & \xi L \le x \le L \end{cases} \tag{46}$$

where

$$C_1 = C_1' \Delta\phi_{\max} = -\frac{\xi L}{2}\Delta\phi_{\max}$$

$$C_2 = C_2' \Delta\phi_{\max} = \left(\frac{\xi^2 L^2}{3} + \frac{L^2\xi^3}{8(1-2\xi)} + \frac{L^2}{(1-\xi)(1-2\xi)}\left(-\frac{5\xi^4}{24} + \frac{\xi^3}{2} - \frac{3\xi^2}{4} + \frac{\xi}{2} - \frac{1}{8}\right)\right)\Delta\phi_{\max}$$

$$C_3 = C_3' \Delta\phi_{\max} = \frac{L}{(1-\xi)}\left(\frac{\xi^2}{2} - \xi\right)\Delta\phi_{\max}$$

$$C_4 = C_4' \Delta\phi_{\max} = \left(\frac{L^2\xi^3}{8(1-2\xi)} + \frac{L^2}{(1-\xi)(1-2\xi)}\left(\frac{11\xi^4}{24} - \frac{5\xi^3}{6} - \frac{\xi^2}{4} + \frac{\xi}{2} - \frac{1}{8}\right)\right)\Delta\phi_{\max}$$

Substituting Eq. (46) into $v_m(x) = k_m S_t(x)$ and integrating the equation twice with respect to *x*, the moment in the steel plates can be derived.

$$\begin{cases} M_{p1}(x) = k_m(\dfrac{x^5}{120\xi L} + \dfrac{C_1' x^3}{6} + \dfrac{C_2' x^2}{2})\Delta\phi_{\max} & 0 \le x \le \xi L \\ M_{p2}(x) = k_m(\dfrac{1}{(1-\xi)L}(\dfrac{Lx^4}{24} - \dfrac{x^5}{120} - \dfrac{L^4 x}{8} + \dfrac{11L^5}{120}) + \dfrac{C_3'}{2}(\dfrac{x^3}{3} - L^2 x + \dfrac{2L^3}{3}) + C_4'(\dfrac{x^2}{2} - Lx + \dfrac{L^2}{2}))\Delta\phi_{\max} & \xi L \le x \le L \end{cases} \quad (47)$$

At the loading point, the maximum curvature difference ($\Delta\phi_{\max}$) between the steel plates and RC beam is obtained by solving the moment equilibrium equation, and expressed as:

$$\Delta\phi_{\max} = \frac{(1-\xi)\xi FL - T_{m,tfi}(\xi L) i_{cp}}{E_c I_c} \frac{1}{(1+\dfrac{1}{\eta})\dfrac{k_m(\dfrac{(\xi L)^4}{120} + \dfrac{C_1'(\xi L)^3}{6} + \dfrac{C_2'(\xi L)^2}{2})}{E_c I_c} + (1-\eta)} \quad (48)$$

The strain and curvature factors can be determined from Eqs. (26) and (39)-(41) with the maximum curvature difference, the force in the bolt in the longitudinal direction and the moment distribution in the steel plates.

2.5. Partial interaction under uniformly distributed loading

A simply supported BSP beam under a uniformly distributed load is shown in Fig. 2(c). Due to the symmetry, only the formulation for the left half of the beam is provided.

The cross-sectional moment with a distance of x from the left support is:

$$M(x) = \frac{mL}{2}x - \frac{mx^2}{2} \quad (49)$$

The boundary and continuity conditions are:

$$\begin{cases} T_{m,tfi}(0) = 0 \\ T_{m,tfi}(L) = 0 \end{cases} \quad (50)$$

The force in the bolt in the longitudinal direction is:

$$T_{m,tfi}(x) = \frac{mq(Lx - x^2)}{2p^2} \tag{51}$$

Assuming that there is linear variation, the difference in the curvature is:

$$\Delta\phi(x) = \frac{2\Delta\phi_{\max}}{L} x \tag{52}$$

The transverse slip can be derived based on the boundary and continuity conditions, and expressed as:

$$S_t(x) = (\frac{x^3}{3L} - \frac{Lx}{4} + \frac{5L^2}{96})\Delta\phi_{\max} \tag{53}$$

Substituting Eq. (53) into $v_m(x) = k_m S_t(x)$ and integrating the equation twice with respect to *x*, the moment in the steel plates can be derived as:

$$M_p(x) = k_m(\frac{x^5}{60L} - \frac{Lx^3}{24} + \frac{5L^2x^2}{192})\Delta\phi_{\max} \tag{54}$$

At the loading point, the maximum curvature difference ($\Delta\phi_{\max}$) between the steel plates and RC beam is obtained by solving the moment equilibrium equation:

$$\Delta\phi_{\max} = \frac{\frac{mL^2}{8} - \frac{mqL^2}{8p^2} i_{cp}}{E_c I_c} \frac{1}{(1+\frac{1}{\eta})\frac{7k_m L^4}{3840E_c I_c} + (1-\eta)} \tag{55}$$

With the maximum curvature difference, the force in the bolt in the longitudinal direction and the moment distribution in the steel plates, the strain and curvature factors can be determined from Eqs. (26), and (39)-(41).

3. Flexural capacity models

3.1. Rigid plastic analysis

Assuming that each component (the RC beam and steel plate) can reach their ultimate load capacity means that the longitudinal reinforcing bars and the entire

section of bolted steel plates have reached their yield strength with a neutral axis identical to that of the RC beam, as shown in Fig. 6. Using the equivalent rectangular concrete compressive stress block described in ACI 318-14 [21], the upper-bound flexural capacity can be determined from the RPA described herein.

First, the neutral axis position is derived from the equilibrium axial load, as shown in Eq. (56). Note that different values of coefficient A_1 should be adopted in accordance with the neutral axis position.

$$0=\alpha f_c \beta x_c + f_{ys} A_{sc} - f_{ys} A_{st} + A_1 \tag{56}$$

where α and β are the coefficients of the equivalent rectangular stress block, f_c is the cylinder compression strength, x_c is the compressive depth, f_{ys} is the yield stress of the steel bar, A_{sc} is the compressive area of the steel bar and A_{st} is the tensile area of the steel bar and A_1 is given as:

$$A_1 = \begin{cases} -f_{yp} A_p & x_c < H - h_p \\ 2 f_{yp} t_p (h_p - (H - x_c)) - 2 f_{yp} t_p (H - x_c) & x_c \geq H - h_p \end{cases} \tag{57}$$

where f_{yp} is the yield stress of the steel plate, t_p is the thickness of the steel plate and h_p is the depth of the steel plate.

Second, the upper-bound flexural capacity can be obtained from Eq. (58).

$$M_{Rigid} = \alpha f_c \beta x_c (H - 0.5\beta x_c) + f_{ys} A_{sc} (H - d_c) - f_{ys} A_{st} d_c + A_2 \tag{58}$$

where M_{Rigid} is the moment capacity derived from the RPA, H is the depth of the

RC beam, d_c is the center of the tensile longitudinal steel bar to the extreme tensile fiber, and A_2 is given as:

$$A_2 = \begin{cases} -0.5 f_{yp} A_p h_p & x_c < H - h_p \\ f_{yp} t_p (h_p - H + x_c)(H - x_c + h_p) - f_{yp} t_p (H - x_c)^2 & x_c \geq H - h_p \end{cases} \quad (59)$$

3.2. Modified moment capacity equations (MMCE) with two factor approach

Due to the longitudinal and partial transverse interactions, the curvature and longitudinal strain profiles of the RC beams and bolted steel plates are different when the BSP beams reach their ultimate limit state. Based on the derived strain and curvature factors, the strain field and hence the stress field in the steel plates can be determined. Assuming that the concrete strain in the extreme compressive fiber reaches its ultimate strain ε_{cu}, the curvature of the RC beam in the ultimate limit state can be obtained from the depth of the neutral axis and the ultimate strain, as follows.

$$\phi_c = \frac{\varepsilon_{cu}}{x_c} \quad (60)$$

The concrete strain at the centroid of the steel plates is given by:

$$\varepsilon_{pc,c} = \phi_c (d_p - x_c) \quad (61)$$

According to the definition of the two factors, the curvature and steel plate strain at the centroid of the steel plate in the ultimate limit state can be determined as follows.

$$\phi_p = \alpha_\phi \frac{\varepsilon_{cu}}{x_c} \quad (62)$$

$$\varepsilon_{pc,p} = \alpha_\varepsilon \phi_c (d_p - x_c) \quad (63)$$

Once the curvature of the plate and strain at the centroid have been determined,

the neutral axis (Eq. (64)), strain and hence the stress distribution can be derived:

$$x_p = \frac{h_p}{2} - \frac{\alpha_\varepsilon}{\alpha_\phi}(d_p - x_c) \tag{64}$$

where x_p is the compressive depth of the steel plate.

The contribution from the steel plates to flexural strength can, therefore, be quantified with the effects of transverse and partial longitudinal interactions. The details of the formulation are provided below.

First, it is assumed that $x_p \geq 0$, which means that the neutral axis of the steel plate is within the depth of the bolted steel plates. Furthermore, depending on whether the bottom tensile fibers of the steel plate have yielded, as shown in Fig. 7, different coefficient values A_3 and A_4 should be adopted in Eqs. (65) and (66).

$$0 = \alpha f_c \beta x_c + f_{ys} A_{sc} - f_{ys} A_{st} + t_p E_p \phi_p x_p{}^2 - A_3 \tag{65}$$

$$M_{partial} = \alpha f_c \beta x_c (H - 0.5\beta x_c) + f_{ys} A_{sc} (H - d_c) - f_{ys} A_{st} d_c + t_p E_p \phi_p x_p{}^2 (h_p - \frac{1}{3} x_p) - A_4 \tag{66}$$

where A_3 and A_4 are given as follows:

$$A_3 = \begin{cases} t_p E_p \phi_p (h_p - x_p)^2 & \varepsilon_{bp} < \varepsilon_{py} \\ 2 f_{yp} t_p (h_p - x_p) - t_p f_{yp} \dfrac{\varepsilon_{yp}}{\phi_p} & \varepsilon_{bp} \geq \varepsilon_{py} \end{cases}$$

and

$$A_4 = \begin{cases} \dfrac{1}{3} t_p E_p \phi_p (h_p - x_p)^3 & \varepsilon_{bp} < \varepsilon_{py} \\ f_{yp} t_p (h_p - x_p)^2 - t_p f_{yp} \dfrac{\varepsilon_{yp}}{\phi_p} (h_p - x_p - \dfrac{1}{3} \dfrac{\varepsilon_{yp}}{\phi_p}) & \varepsilon_{bp} \geq \varepsilon_{py} \end{cases}$$

where ε_{bp} is the steel plate strain at the bottom of the steel plate and ε_{py} is the yield strain of the steel plate.

Second, it is assumed that $x_p < 0$, i.e. the neutral axis of the steel plate is not within the depth of the bolted steel plates. Similar to the above circumstances,

depending on whether the bottom tensile fibers of the steel plate have yielded yet, different coefficient values of A_5 and A_6 should be used in Eqs. (67) and (68) as shown in Fig. 8.

$$0 = \alpha f_c \beta x_c + f_{ys} A_{sc} - f_{ys} A_{st} + A_5 \tag{67}$$

$$M_{partial} = \alpha f_c \beta x_c (H - 0.5\beta x_c) + f_{ys} A_{sc} (H - d_c) - f_{ys} A_{st} d_c - A_6 \tag{68}$$

where A_5 and A_6 are:

$$A_5 = \begin{cases} 2t_p E_p (\varepsilon_{cp,p} + \phi_p \frac{h_p}{2}) h_p - t_p E_p \phi_p h_p^2 & \varepsilon_{bp} < \varepsilon_{py} \\ 2 f_{yp} t_p h_p - \frac{t_p E_p (\varepsilon_{py} - (\varepsilon_{cp,p} - 0.5 h_p \phi_p))^2}{\phi_p} & \varepsilon_{bp} \geq \varepsilon_{py} \end{cases}$$

and

$$A_6 = \begin{cases} t_p E_p (\varepsilon_{cp,p} + \phi_p \frac{h_p}{2}) h_p^2 - \frac{2}{3} t_p E_p \phi_p h_p^3 & \varepsilon_{bp} < \varepsilon_{py} \\ f_{yp} t_p h_p^2 - \frac{t_p E_p (\varepsilon_{py} - (\varepsilon_{cp,p} - 0.5 h_p \phi_p))^2}{\phi_p} (h_p - \frac{1}{3} \frac{(\varepsilon_{py} - (\varepsilon_{cp,p} - 0.5 h_p \phi_p))}{\phi_p}) & \varepsilon_{bp} \geq \varepsilon_{py} \end{cases}$$

4. Comparison with available test results

To validate the proposed model, the predicted strain factor and flexural capacity were compared with available results on tests carried out on BSP beam samples under four point-bending [1-3]. The test results were selected on the basis that the centroid of the steel plate should be lower than that of the RC beam to justify the assumption made for Eq. (7). Details on the material and geometric parameters of the samples are summarized in Table 1. The definitions of the geometric parameters are shown in Fig. 9.

The strain factors (α_ε) at the loading point derived from the proposed method are compared with those in Su et al. [17] in Fig. 10. It can be seen that the strain factors obtained by Su et al. [17] are consistently higher than those obtained in this paper.

Therefore, Su et al. [17] could have overestimated the load carrying capacity of the BSP beams because they did not consider the effect of the partial transverse interaction.

The flexural capacities derived from the RPA and MMCE are summarized in Table 2. Note that both the strain factors determined in accordance with the method in Su et al. [17] and the proposed method are used to derive the flexural capacity. As shown in Table 2, the flexural capacity determined by the RPA substantially overestimates the test results except for the SBWP and WBWP samples because the entire steel plate at the critical section of these two samples yielded which corresponds to the assumption made for the RPA and the same capacity is derived. Except for these two samples, the discrepancies of the MMCEs are substantially less than those of the RPA. Furthermore, the mean predicted capacity to calculate the capacity ratios determined by the MMCEs from the approach here and that in Su et al. [17] is 1.05 and 1.10, respectively, while that determined by the RPA is 1.15. The results show that neglecting the effect of the partial transverse interaction results in a higher strain factor and an overestimated moment capacity. Hence, the method in this study which takes partial transverse interaction into consideration can indeed improve the accuracy of the predicted flexural capacity of BSP beams.

5. Design recommendations for BSP beams

5.1. Strain and curvature factors

Using higher strain and curvature factors can reduce partial interaction and increase the flexural capacity of BSP beams. Nevertheless, the level of enhancement of flexural capacity with increased strain or curvature factors should be further investigated. In order to find a balance between the strengthening effect (satisfactory

strength enhancement) and strengthening efficiency (an economic number of bolts), a parametric study is conducted with ten selected samples from the literature [1-3]. The normalized flexural capacity (γ_M) is defined as follows:

$$\gamma_M = \frac{M' - M_0}{M_1 - M_0} \tag{69}$$

where M_1 is the flexural capacity when the strain or curvature factor is taken as 1.0, while M_0 is the flexural capacity with strain or curvature factor is taken as zero and M' is the flexural capacity with other values of strain or curvature factors.

Fig. 11 shows that the normalized flexural capacity varies with the strain and curvature factors. The flexural capacity increases with increases in the strain and curvature factors. When the normalized flexural capacity reaches 0.9 the strain or curvature factor is 0.7. Further increases in the strain or curvature factor will only result in a small increase in the flexural capacity. Thus a strain and curvature factor of 0.7 allows both a strengthening effect and strengthening efficiency.

5.2. Normalized bolt stiffness

The strain and curvature factors are influenced by the parameters, including the span-to-depth ratio (*L/H*) of the RC beam, ratio of the steel plate to the flexural stiffness of the RC beam, axial stiffness of steel plate and bolt stiffness. After conducting a comprehensive parametric study, the strain and curvature factors are found to be more sensitive to the span-to-depth ratio of the RC beam and the normalized bolt stiffness γ_{bolt} which is defined as:

$$\gamma_{bolt} = \frac{k_m d_p^{\,2}}{E_p A_p} \tag{70}$$

A total of 18 model beams with various span-to-depth ratios and normalized bolt stiffnesses were used to examine the relation between the strain and curvature factors

and normalized bolt stiffness. The key parameters of the modeled beams are presented in Table 3. The effects of three cases of loading as shown in Fig. 2 together with the considered three different aspect ratios (10.3, 6.9 and 3.4). Fig.12 plots the strain or curvature factors against normalized bolt stiffness. The minimum normalized bolt stiffness to achieve the strain and curvature factors of 0.7 was determined. Obviously, the normalized bolt stiffness derived from the strain factor in Fig. 12(a) is greater than that from the curvature factor in Fig. 12(b). Thus the normalized bolt stiffness from the strain factor would control the limiting values. The normalized bolt stiffness are found to be 0.13, 0.17 and 0.21 from Fig. 12(a) for the three cases of loading as shown in Figs. 2(a), 2(b) and 2(c). The distributed loading case often works together with another concentrated loading case (either three-point bending or four point bending). Hence, to simplify the design, a relative conservative value of 0.2 is used for the BSP beam to satisfy the strengthening effect and strengthening efficiency. This normalized bolt stiffness value can ensure enhanced capacity and provides a reference for engineers to determine the number of required bolts in a design.

5.3. Depth of steel plate

The level of enhanced flexural capacity with the use of BSP beams is affected by the depth, thickness and position of the bolted steel plates. Therefore, the dimensions of the steel plates should be appropriately determined in a strengthening design. In this study, the bottom edge of the steel plate is aligned with the beam soffit to maximize the flexural capacity of the BSP beams. A parametric study is then conducted to investigate the effects of the following parameters: the ratio of the thickness of the steel plate to the depth of the RC beam (γ_t=100t_p/H), the ratio of the depth of the steel plate to the depth of the RC beam cross-section (γ_d), and the tensile

steel ratio (ρ_s). The ranges of the parameters are shown in Table 4. The enhanced moment capacity ratio γ_m is defined as:

$$\gamma_m = \frac{0.9M_{BSP} - M_{RC}}{M_{RC}} \tag{71}$$

where M_{BSP} is the moment capacity of the BSP beam derived by assuming full interaction and M_{RC} is the moment capacity of the original RC beam. The coefficient of 0.9, which represents the normalized strength enhancement coefficient, is introduced according to Fig. 11 when the strain and curvature factors reached 0.7 and the normalized bolt stiffness is not less than 0.2 as shown in Fig. 12.

It can be seen from Fig. 13 that the enhanced moment capacity ratio decreases with increased depth of the RC beam cross-section and the tensile reinforcement ratio, but increases with plate thickness and plate depth to the beam depth ratio. Hence, the enhanced moment capacity that can be achieved for a BSP beam with greater depth and a high tensile reinforcement ratio is limited. Thick plates that are placed with depth are more effective for strengthening RC beams. Furthermore, the enhanced moment capacity ratio is plotted against the ratio of the thickness of the plate to the depth of the beam (γ_t). By using the least squares method, the formula for determining the depth of a steel plate can be derived:

$$\gamma_m = (1.38\gamma_t - 0.05)e^{(3\gamma_d)^{0.33}(-141\rho_s + 0.65)} \tag{72}$$

Fig. 14 is a comparison of the predicted enhanced moment capacity ratio with that derived from Eq. (72), and there is good agreement. Rearranging Eq. (72),

$$\gamma_d = \frac{1}{3}\left(\frac{1}{-141\rho_s + 0.65}\right)^3 \left(\ln\frac{\gamma_m}{1.38\gamma_t - 0.05}\right)^3 \tag{73}$$

Eq. (73) can be used for a quick estimation of the required depth of the steel plate. It should be noted that this formula can only be used when the enhancement moment ratio is less than 2.5.

5.4. Simplified design procedure for BSP beams

The parametric study described above can be applied to develop a simplified design procedure for BSP beams. The key steps are as follows.

(1) The moment capacity of the original RC beam can be derived in accordance with the geometry and reinforcement arrangement of the RC beam. An enhanced flexural capacity ratio is determined to satisfy the specific requirements of the moment capacity. The steel plate dimensions (h_p and t_p) can be obtained by referring to Fig. 13 and Eq. (73).

(2) Assuming that the bottom edge of the steel plate is aligned with the beam soffit, the depth of the centroid of the steel plate to the extreme compressive fiber of the RC beam can be determined with $d_p = H - 0.5h_p$.

(3) By applying both a strain and curvature factor of 0.7 and normalized bolt stiffness (γ_{bolt}) of 0.2, the distributed bolt stiffness (k_m) can be determined with:

$$k_m = \frac{0.2E_pA_p}{d_p^{\,2}} \tag{74}$$

(4) To avoid connection failure, the steel plates should be designed to yield prior to the yielding of bolts, which means that the shear capacity of the bolts should be greater than the yield strength of the steel plate. Hence, the following relationship should be satisfied.

$$nR_{by} \geq f_{yp} t_p h_p \tag{75}$$

where n is the minimum number of bolts on each shear span to fix the steel plate.

(5) Since the material properties (E_p and f_{yp}), dimensions (h_p and t_p), required distributed bolt stiffness (k_m) and depth of the centroid of the steel plate to the extreme compressive fiber (d_p) have been derived, the shear strength of the bolt ($R_{by} = k_m S_b S_{by}$), minimum number of bolts on each face of the shear span (n) and the bolt spacing (S_b) can be determined with Eqs. (74) and (75).

6. Conclusion

In this paper, a flexural capacity design model is proposed, which takes into account the partial transverse interaction of BSP beams. The effect of partial transverse interaction on longitudinal strain slip which will increase the latter is incorporated into this theoretical model. The conclusions are as follows.

(1) By comparing the predicted flexural capacity and available test results, it can be concluded that MMCEs are more appropriate for estimating the capacity of BSP beams. Furthermore, the theoretical model proposed in this paper that takes into consideration both longitudinal and partial transverse interactions is more accurate than the model in Su et al. [17].

(2) The enhanced flexural capacity ratio is reduced with increases in the depth of the RC beam cross-section and tensile reinforcement ratio, but is increased with increases in the thickness and depth of the plate to the beam depth ratio (γ_d).

(3) To obtain both an optimal strengthening effect and strengthening efficiency, the

strain and curvature factors are both 0.7.

(4) To ensure that the strain and curvature factors will not be less than 0.7, the normalized bolt stiffness (γ_{bolt}) is a conservative 0.2.

(5) Lastly, it is worthy to mention that the proposed theoretical model is also applicable to RC beams strengthened with bottom plate.

References

[1] Li LZ, Lo SH, Su RKL. Experimental study of moderately reinforced concrete beams strengthened with bolted-side steel plates. Adv Struct Eng 2013;16(3):499-516.

[2] Su RKL, Siu WH, Smith ST. Effects of bolt–plate arrangements on steel plate strengthened reinforced concrete beams. Eng Struct 2010;32(6): 1769-1778.

[3] Ahmed M, Oehlers DJ, Bradford MA. Retrofitting reinforced concrete beams by bolting steel plates to their sides-Part 1: Behaviour and experiments. Struct Eng Mech 2000;10(3):211-226.

[4] Cheng B, Su RKL. Retrofit of deep concrete coupling beams by a laterally restrained side plate. J Struct Eng ASCE 2010;137(4):503-512.

[5] Jiang CJ, Lu ZD, Li LZ. Shear performance of fire-damaged reinforced concrete beams repaired by a bolted side-plating technique. J Struct Eng ASCE 2017;143(5):04017007.

[6] Li LZ, Cai ZW, Lu ZD, Zhang XL, Wang, L. Shear performance of bolted side-plated reinforced concrete beams. Eng Struct 2017;144(8):73-87.

[7] Nguyen NT, Oehlers DJ, Bradford MA. An analytical model for reinforced concrete beams with bolted side plates accounting for longitudinal and transverse partial interaction. Int J Solids Struct 2001;38(38):6985-6996.

[8] Oehlers DJ, Nguyen NT, Ahmed M, Bradford MA. Transverse and longitudinal partial interaction in composite bolted side-plated reinforced-concrete beams. Struct Eng Mech 1997;5(5):553-563.

[9] Oehlers DJ, Ahmed M, Nguyen NT, Bradford MA. Retrofitting reinforced concrete beams by bolting steel plates to their sides-Part 2: transverse interaction and rigid plastic design. Struct Eng Mech 2002;10(3): 227-243.

[10] Siu WH, Su RKL. Effects of plastic hinges on partial interaction behaviour of bolted side-plated beams. J Constr Steel Res 2010;66(5): 622-633.

[11] Su RKL, Cheng B. Plate-strengthened deep reinforced concrete coupling beams. P I Civil Eng-Str B 2011.

[12] Su RKL, Zhu Y. Experimental and numerical studies of external steel plate strengthened reinforced concrete coupling beams. Eng Struct 2005;27(10):1537-1550.

[13] Yuan LP. Partial interaction behaviour of bolted side plated reinforced concrete beams. PHD dissertation. Adelaide: University of Adelaide; 2003.

[14] Zhu Y, Su RKL. Behavior of strengthened reinforced concrete coupling beams by bolted steel plates, Part 2: Evaluation of theoretical strength. Struct Eng Mech 2010;34(5):563.

[15] Zhu Y, Su RKL, Zhou FL. Seismic behavior of strengthened reinforced concrete coupling beams by bolted steel plates, Part 1: Experimental study. Struct Eng Mech 2007;27(2):149-172.
[16] Nguyen NT, Oehlers DJ, Bradford MA. A rational model for the degree of interaction in composite beams with flexible shear connectors. Journal of Structural Mechanics 1998;26(2):175-194.
[17] Su RKL, Li LZ, Lo SH. Longitudinal partial interaction in bolted side-plated reinforced concrete beams. Adv Struct Eng 2014;17(7): 921-936.
[18] Li LZ, Jiang CJ, Su RKL, Lo SH. A piecewise linear transverse shear transfer model for bolted side-plated beams. Struct Eng Mech 2017;62(4):443-453.
[19] Su RKL, Li LZ, Lo SH. Shear transfer in bolted side-plated reinforced concrete beams. Eng Struct 2013;56:1372-1383.
[20] Lo SH, Li LZ, Su RKL. Optimization of partial interaction in bolted side-plated reinforced concrete beams. Comput Struct 2014;131:70-80.
[21] ACI 318-14. Building Code Requirements for Structural Concrete and Commentary, USA: American Concrete Institute; 2014.

Notations

ε_{RC}	strain in RC beam
ε_p	strain in steel plate
ϕ_p	curvature of steel plate in partial transverse interaction
ϕ_c	curvature of RC beam in partial transverse interaction
S_l	longitudinal slip
S_t	transverse slip
M	total moment in one section
M_p	moment in steel plate
M_c	moment in RC beam
V	total shear in one section
V_c	shear in RC beam
V_p	shear in steel plate
t_m	longitudinal shear flow
v_m	transverse shear flow
i_{cp}	distance between centroids of RC beam and steel plate
$\varepsilon_{cc,c}$	RC beam strain in centroid of RC beam
$\varepsilon_{pc,c}$	RC beam strain in centroid of steel plate
$\varepsilon_{pc,p}$	steel plate strain in centroid of steel plate
K_b	bolt stiffness
R_{by}	yield shear force of bolt
S_{by}	yield deformation of bolt
S_b	bolt spacing
k_m	distribution stiffness, defined by $\frac{K_b}{S_b}$
E_c	elastic modulus of RC beam
E_p	elastic modulus of steel plate
A_c	cross-section area of RC beam
A_P	cross-section area of steel plate
H	depth of RC beam
B	width of RC beam
h_p	depth of steel plate
d_p	depth of centroid of steel plate to extreme compressive fiber
d_c	center of the tensile longitudinal steel bar to extreme tensile fiber
β	factor relating depth of equivalent rectangular stress block to neutral axis
α	factor relating average stress of equivalent rectangular stress block
x_c	depth of neutral axis of RC beam
f_c	cylinder compressive strength
x_p	compressive depth of steel plate

f_{ys}	yield stress of steel bar
f_{yp}	yield stress of steel plate
A_{sc}	compressive area of steel bar
A_{st}	tensile area of steel bar
ε_{cu}	ultimate strain in RC beam
ε_{bp}	steel plate strain at the bottom of the steel plate
ε_{py}	yield strain of steel plate
α_{ε}	strain factor
α_{ϕ}	curvature factor
t_p	thickness of steel plate
$M_{partial}$	moment capacity derived by partial interaction analysis
M_{Rigid}	moment capacity derived by plastic rigid analysis
L	length of RC beam
F	force exerted by hydraulic jack
x	distance to left support
$\Delta\phi$	difference in curvature in BSP beam
$\Delta\phi_{\max}$	maximum curvature difference in BSP beam
T_m	shear force in bolt along longitudinal direction
V_m	shear force in bolt along transverse direction
T_{m1}	shear force in bolt in shear span
T_{m2}	shear force in bolt in pure bending moment region or in shear span (single point load case)
T_{m1}'	first derivation of T_{m1}
T_{m2}'	first derivation of T_{m2}
S_{t1}	transverse slip in shear span
S_{t2}	transverse slip in pure bending moment region or in shear span (single point load case)
v_{m1}	uniform shear distribution in shear span
v_{m2}	uniform shear distribution in pure bending moment region or in shear span (single point load case)
V_{p1}	shear force of steel plate in shear span
V_{p2}	shear force of steel plate in pure bending moment region or in shear span (single point load case)
M_{p1}	steel plate moment in shear span
M_{p2}	steel plate moment in pure bending moment region or in shear span (single point load case)
M_{p1}'	equal to $M_{p1}/\Delta\phi_{\max}$
M_{p2}'	equal to $M_{p2}/\Delta\phi_{\max}$
$\delta_{pc,p}$	longitudinal displacement in steel plate at centroid of steel plate
$\delta_{pc,c}$	longitudinal displacement in RC beam at centroid of steel plate

ϕ	curvature of full transverse interaction
ε_{et}	extreme tensile fiber of steel plate
F_{test}	tested results
F_{mod}	results derived from modified moment capacity analysis with two proposed factors
F_{PRA}	results derived from plastic rigid analysis
ξ	ratio of distance from loading point to left support to overall length
m	distribution load per unit length
η	ratio of flexural stiffness of steel plate to flexural stiffness of RC beam
F_{Su}	results derived from modified moment capacity analysis with two factors proposed in Su et al. (2014).
γ_{bolt}	normalized bolt stiffness
γ_M	normalized strength enhancement
M_0	moment capacity with strain factor or curvature factor equal to 0
M_1	moment capacity with strain factor or curvature factor equal to 1
M'	moment capacity with strain factor or curvature factor value in 0 to 1
γ_d	ratio of depth of steel plate to depth of RC beam section
γ_m	enhanced moment capacity ratio
ρ_s	longitudinal tensile reinforcement ratio
γ_t	ratio of steel plate thickness to depth of beam
$\gamma_{m,\mathrm{mod}el}$	enhanced flexural capacity ratio derived from fitting function
M_{BSP}	flexural capacity of BSP beam at ultimate limit stage
M_{RC}	flexural capacity of RC beam at ultimate limit stage
n	number of bolts

Table 1 Tested parameters of samples

Source	Sample	H (mm)	B (mm)	d_p (mm)	h_p (mm)	f_c (Mpa)	K_b (N/mm)	S_b (mm)
Li et al. (2013)	P75B300	350	225	250	75	33.9	80000	300
	P100B300	350	225	250	100	28.9	80000	300
	P100B450	350	225	250	100	33.2	80000	450
Siu and Su (2010)	SBSP	350	225	250	150	34.6	80000	400
	WBSP	350	225	250	150	34.3	80000	600
	WBWP	350	225	250	75	35.1	80000	600
	SBWP	350	225	250	75	35.3	80000	300
Ahmed et al. (2000)	B11	370	200	257.5	145	49.2	13929	185
	B12	370	200	257.5	145	49.2	13929	370
	B24	370	200	257.5	145	45.5	13929	370

Table 2 Comparison of flexural strength

Sample	MMCE (kN)		RPA (kN)	F_{test} (kN)	$F_{present}/F_{test}$	F_{Su}/F_{test}	F_{RPA}/F_{test}
	$F_{present}$	F_{Su}					
P75B300	170.8	173.9	178.3	161.5	1.06	1.08	1.10
P100B300	166.3	177.7	177.5	158.5	1.05	1.12	1.12
P100B450	174.9	187.6	186.2	163.3	1.07	1.15	1.14
SBSP	157.5	158.9	166.3	161.5	0.98	0.98	1.03
WBSP	147.0	152.5	166.3	149.2	0.99	1.02	1.11
WBWP	129.4	129.4	129.4	133.4	0.98	0.98	0.98
SBWP	129.4	129.4	129.4	144.6	0.90	0.90	0.90
B11	122.2	130.2	133	101.0	1.21	1.29	1.33
B12	96.3	112.2	133	91.3	1.05	1.23	1.46
B24	112.6	116.7	130.3	97.8	1.15	1.19	1.33
Average:					1.04	1.10	1.15

Table 3 Sample details for parametric study

Sample	L (mm)	t_p (mm)	H (mm)	B (mm)	d_p (mm)	h_p (mm)	f_c (MPa)	K_b (kN/mm)	S_b (mm)
S1	3600	6	350	225	250	100	33.9	10	300
S2	3600	6	350	225	250	100	33.9	20	300
S3	3600	6	350	225	250	100	33.9	40	300
S4	3600	6	350	225	250	100	33.9	80	300
S5	3600	6	350	225	250	100	33.9	160	300
S6	3600	6	350	225	250	100	33.9	240	300
S7	2400	6	350	225	250	100	33.9	10	300
S8	2400	6	350	225	250	100	33.9	20	300
S9	2400	6	350	225	250	100	33.9	40	300
S10	2400	6	350	225	250	100	33.9	80	300
S11	2400	6	350	225	250	100	33.9	160	300
S12	2400	6	350	225	250	100	33.9	240	300
S13	1200	6	350	225	250	100	33.9	10	300
S14	1200	6	350	225	250	100	33.9	20	300
S15	1200	6	350	225	250	100	33.9	40	300
S16	1200	6	350	225	250	100	33.9	80	300
S17	1200	6	350	225	250	100	33.9	160	300
S18	1200	6	350	225	250	100	33.9	240	300

Table 4 Details of parametric study

Parameter	ρ_s	t_p (mm)	H (mm)	γ_t	γ_d
Parameter range	0.005-0.015	3-12	300-800	0.38-2	0.25-0.5

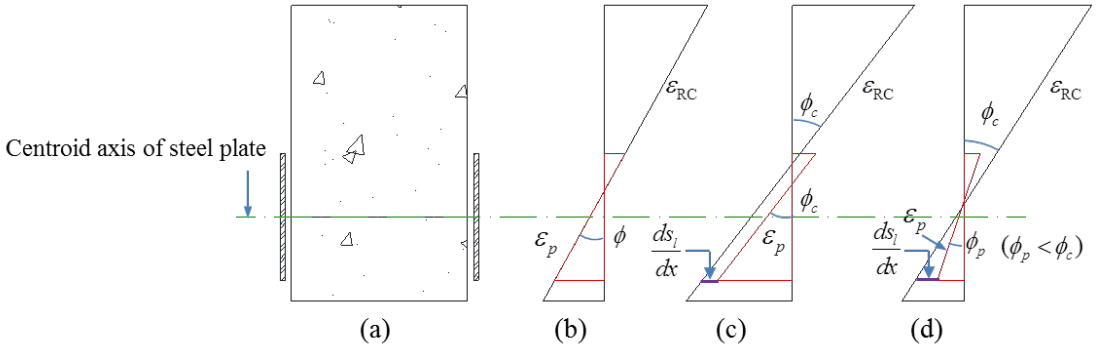

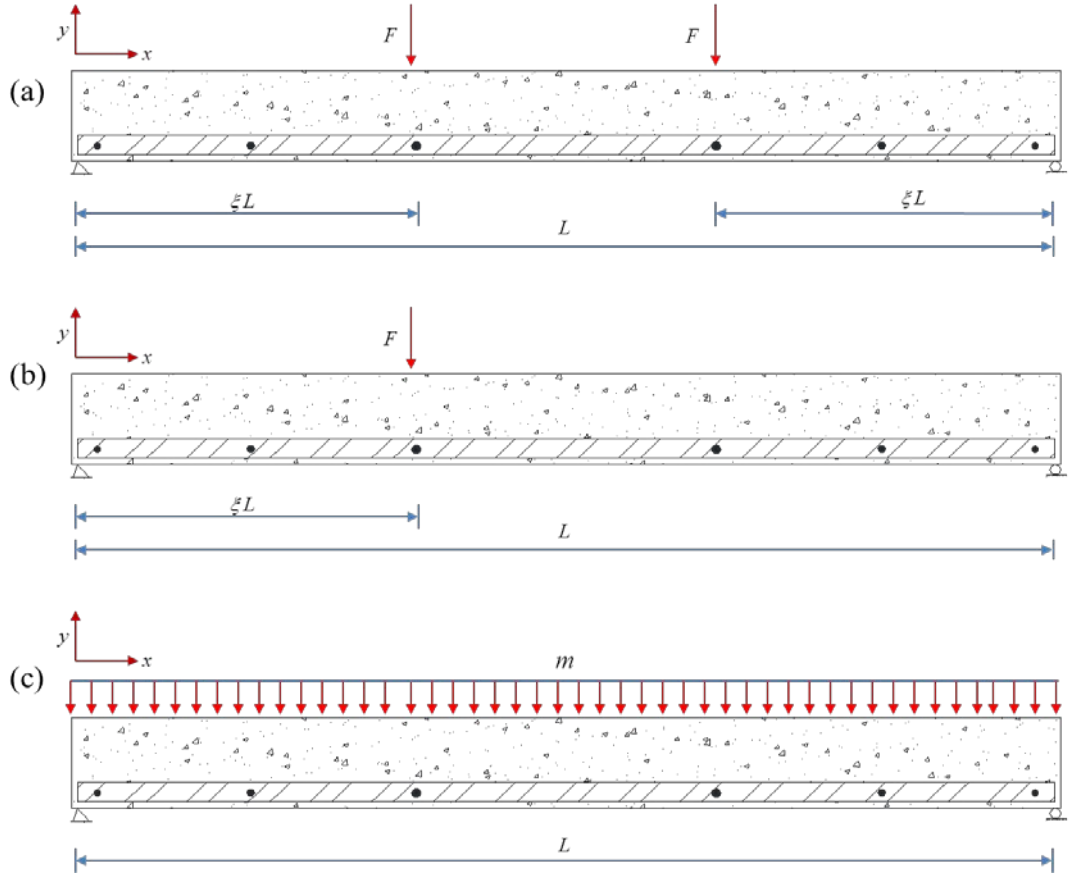

Fig. 2. BSP beams under three loading cases (a) four-point bending, (b) three-point loading and (c) uniform loading

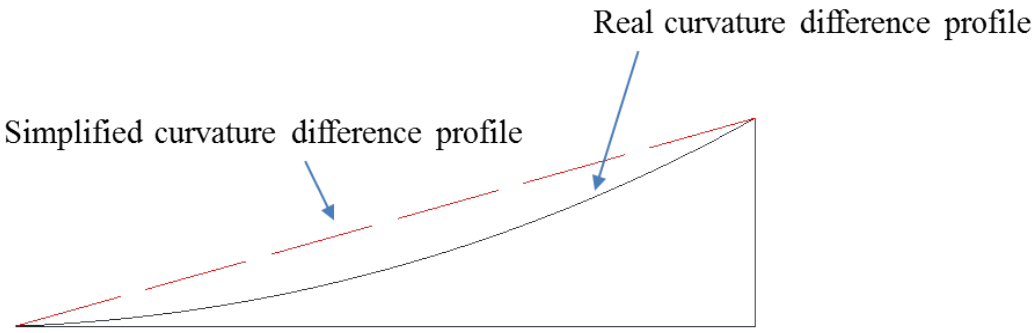
Real curvature difference profile
Simplified curvature difference profile

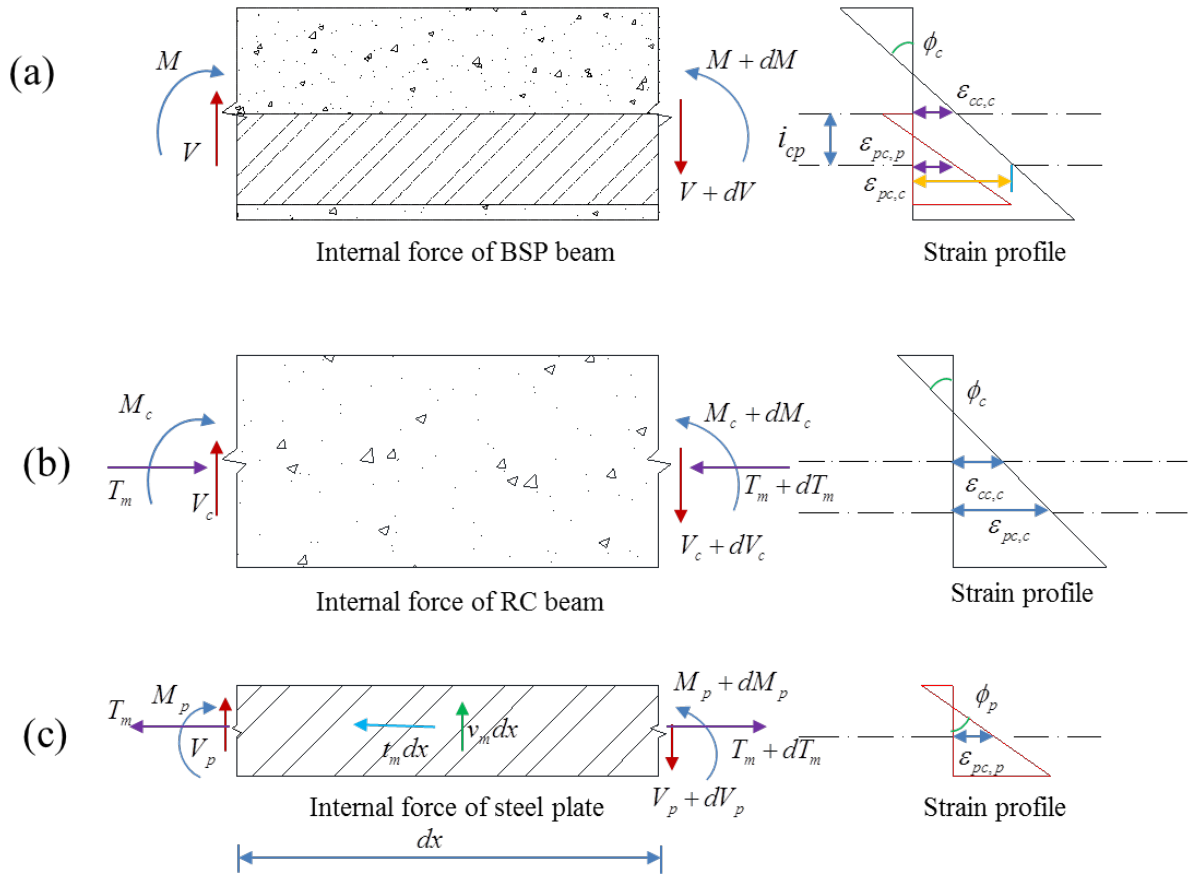

Fig. 4. Internal force and strain profile (a) BSP beam, (b) RC beam and (c) steel plate

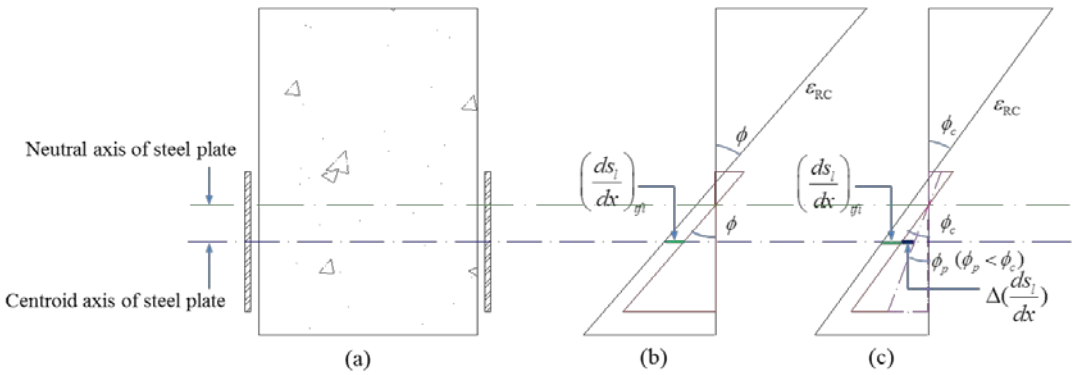

Fig. 5. Effect of partial transverse interaction on longitudinal slip (a) section diagram, (b) full transverse interaction and (c) partial transverse interaction

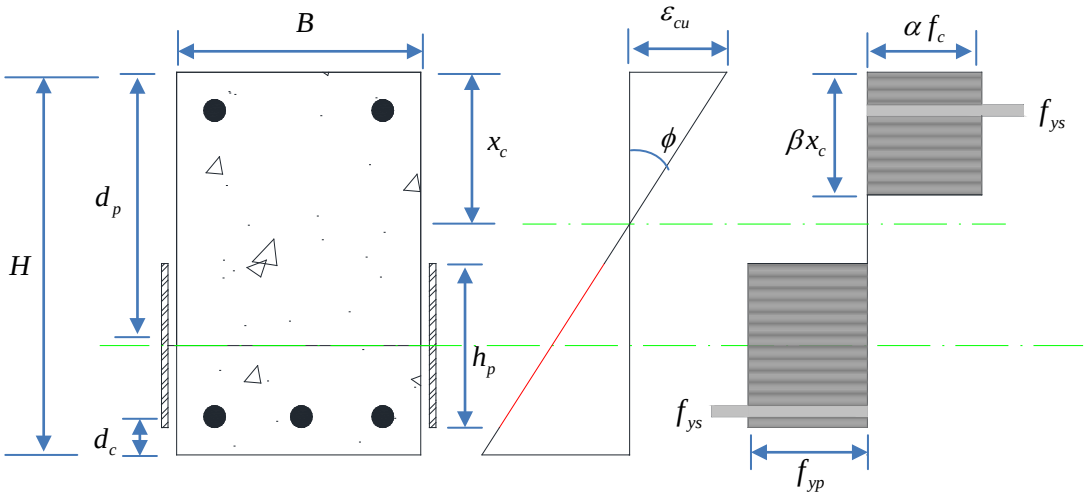
B
H
d_p
d_c
x_c
h_p
ε_{cu}
ϕ
αf_c
βx_c
f_{ys}
f_{yp}

(a) (b) (c)

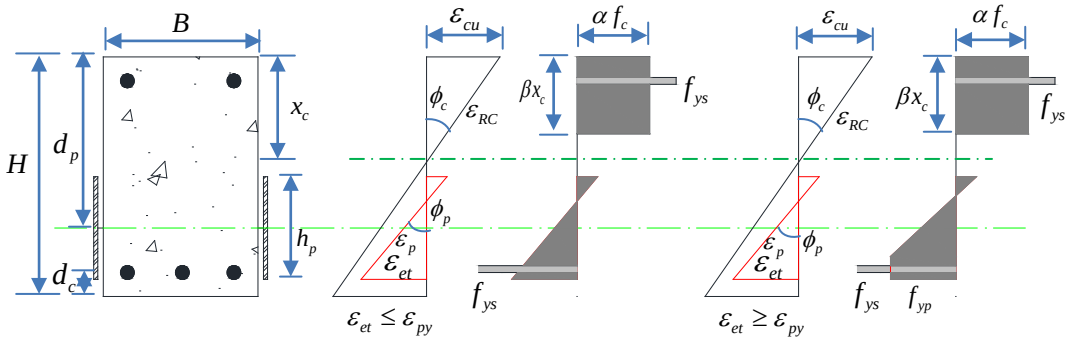
B
H
d_p
d_c
x_c
h_p
ε_{cu}
ϕ_c
ε_{RC}
ϕ_p
ε_p
ε_{et}
αf_c
βx_c
f_{ys}
f_{yp}
$\varepsilon_{et} \le \varepsilon_{py}$
$\varepsilon_{et} \ge \varepsilon_{py}$

(a) (b) (c) (d) (e)

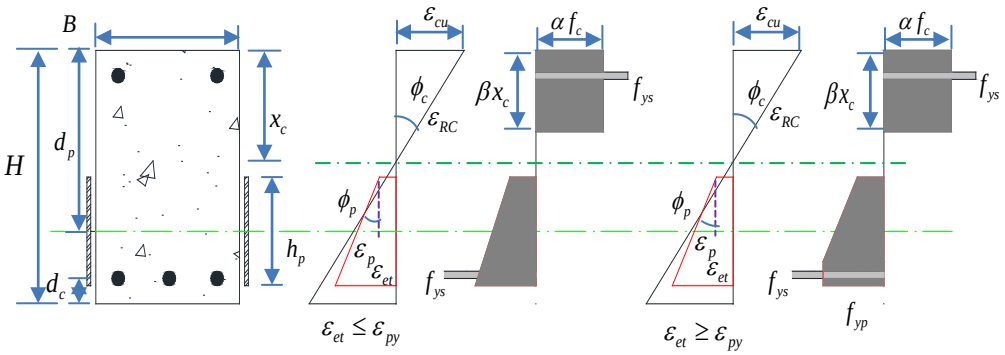
B
H
d_p
d_c
x_c
h_p
ε_{cu}
ϕ_c
ε_{RC}
ϕ_p
ε_p
ε_{et}
$\varepsilon_{et} \le \varepsilon_{py}$
αf_c
βx_c
f_{ys}
$\varepsilon_{et} \ge \varepsilon_{py}$
f_{yp}
(a)
(b)
(c)
(d)
(e)

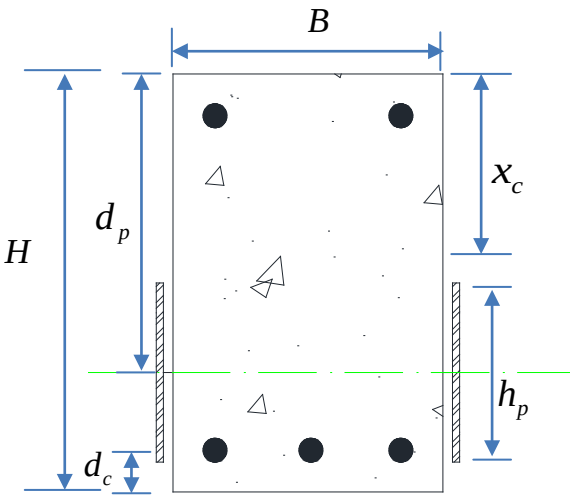
B
H
d_p
d_c
x_c
h_p

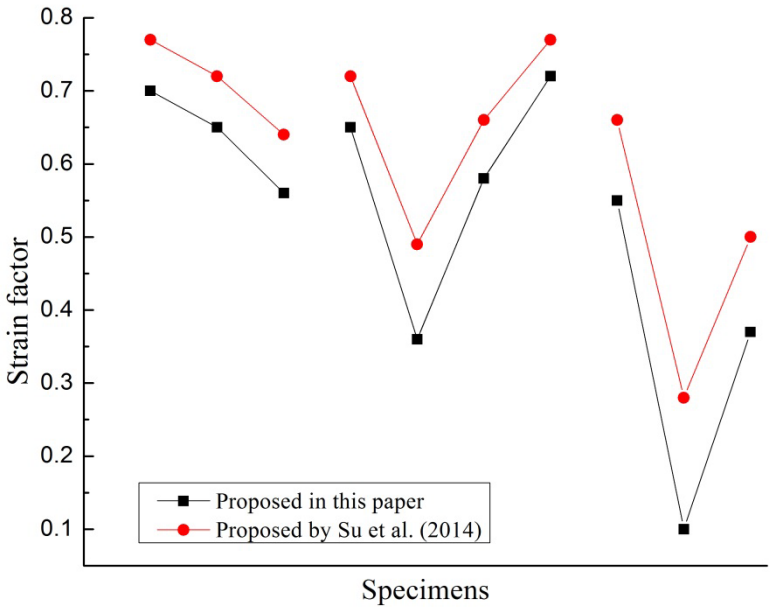
0.8
0.7
0.6
0.5
0.4
0.3
0.2
0.1
Strain factor
Proposed in this paper
Proposed by Su et al. (2014)
Specimens

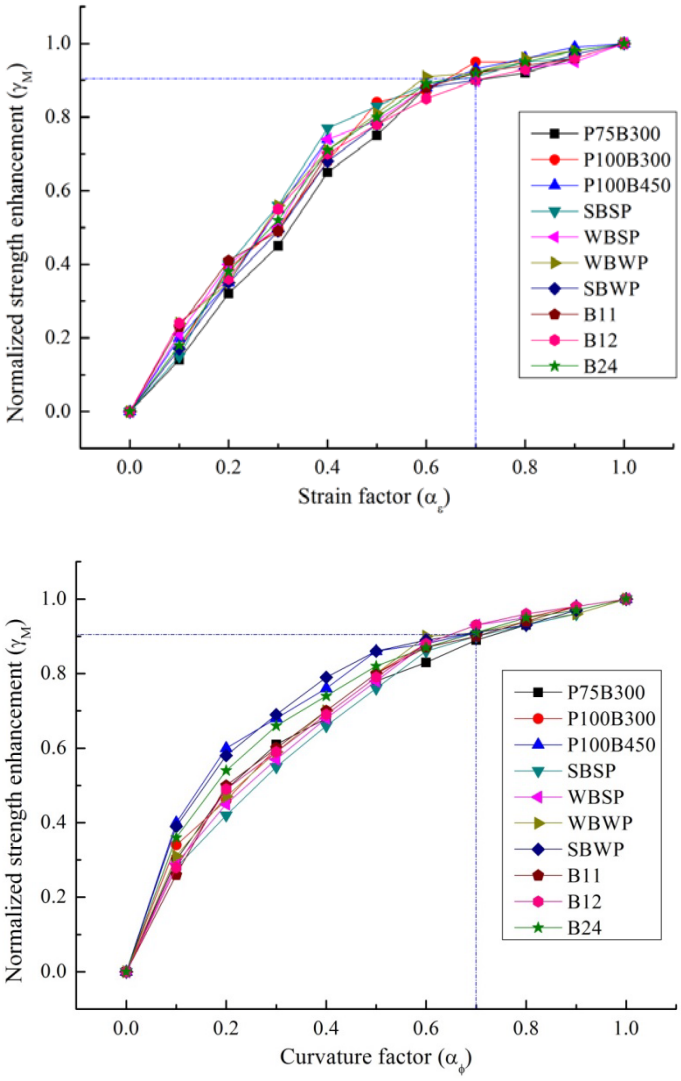

Fig. 11. Normalized strength enhancement with (a) strain factor and (b) curvature factor

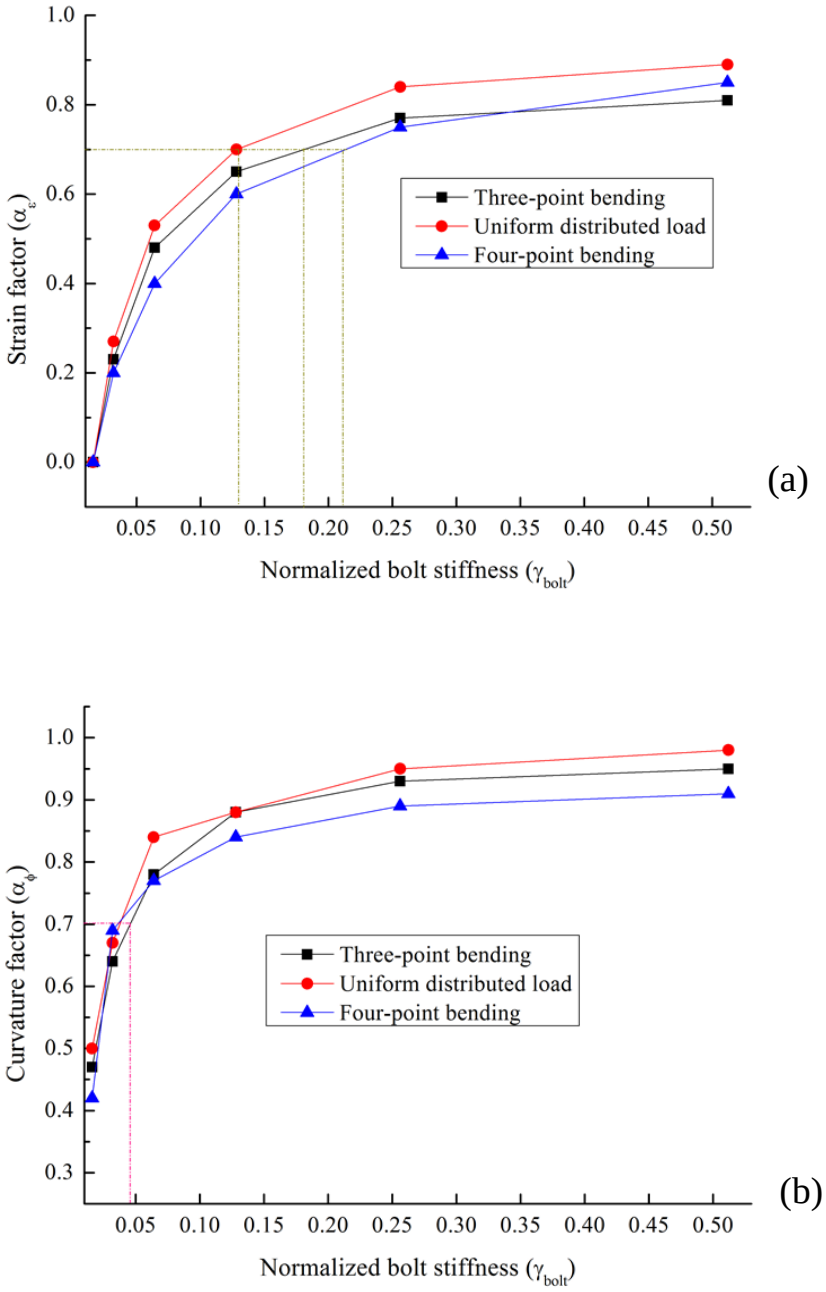

Fig. 12. Normalized bolt stiffness with (a) strain factor and (b) curvature factor

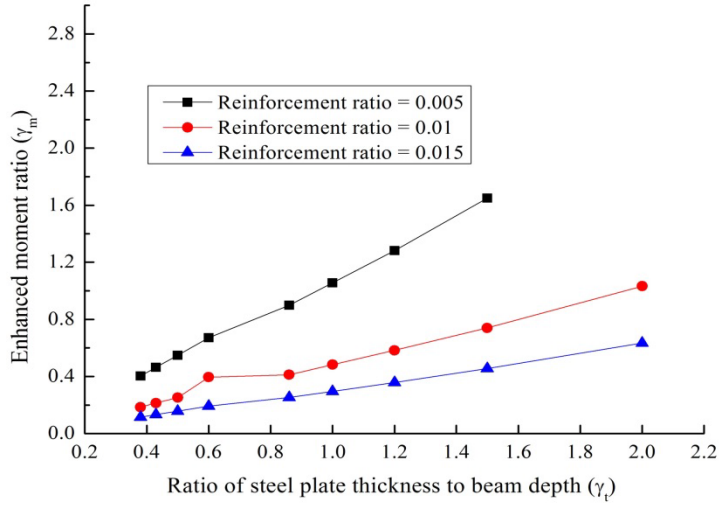

(a)

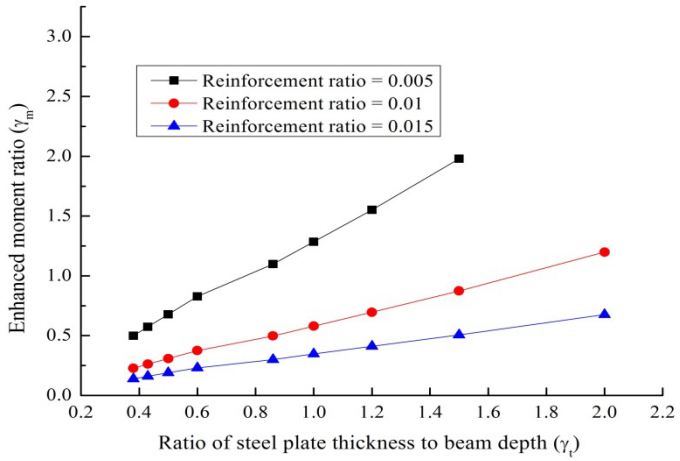

(b)

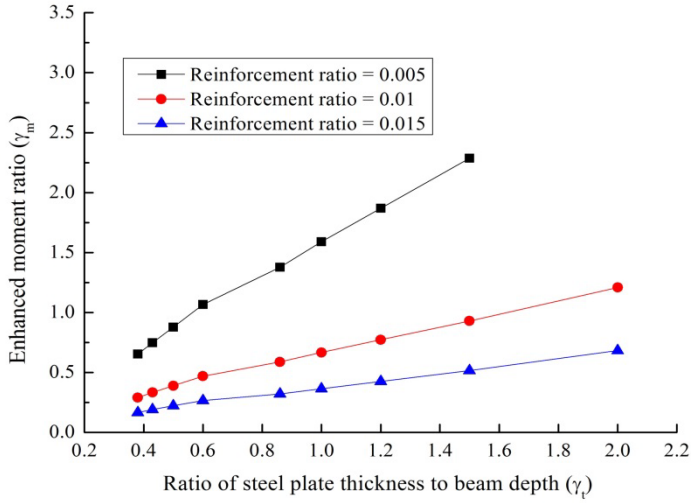

(c)

Fig. 13. Enhanced moment capacity ratios (a) γ_d = 0.25, (b) γ_d = 0.33 and (c) γ_d = 0.5

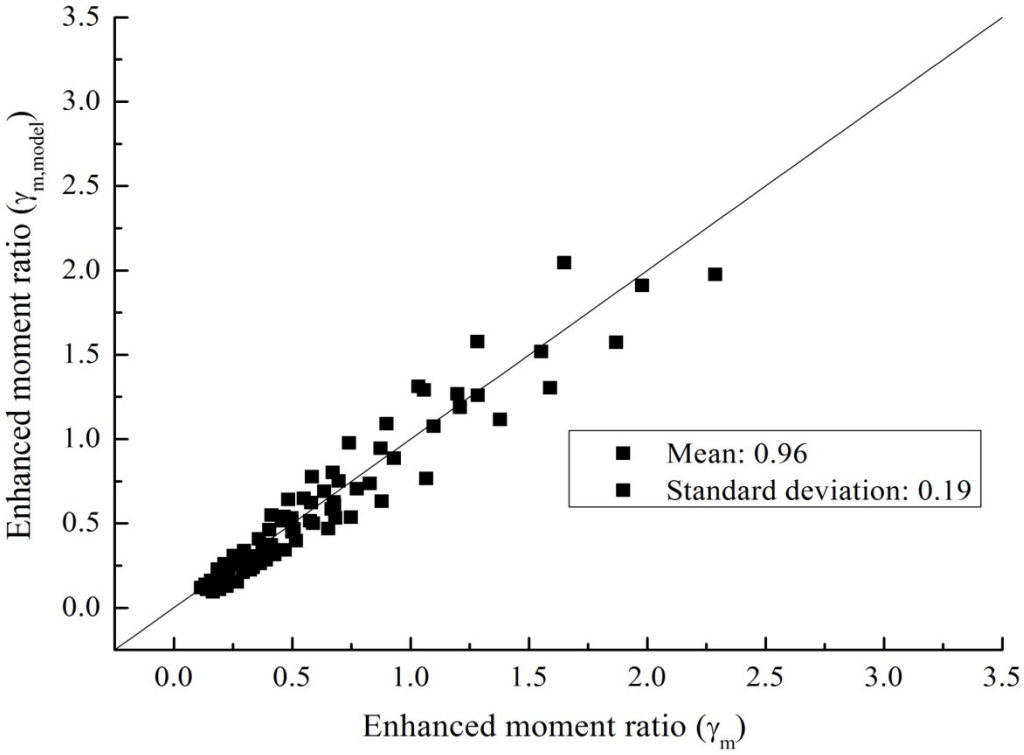

Fig. 14. Comparison of enhanced moment ratio